Theor Chim Acta (1997) 95: 131–150

Theoretica Chimica Acta

Symmetry adaptation and the utilization of point group symmetry in valence bond calculations, including CASVB

Thorstein Thorsteinsson[1,*], David L. Cooper[1], Joseph Gerratt[2], Mario Raimondi[3]

[1] Department of Chemistry, University of Liverpool, P.O. Box 147, Liverpool L69 3BX, UK

[2] School of Chemistry, University of Bristol, Cantocks Close, Bristol BS8 1TS, UK

[3] Dipartimento di Chimica Fisica ed Elettrochimica, Università di Milano, Via Golgi 19, 20133 Milano, Italy

Received October 9, 1996/Final version received November 7, 1996/Accepted November 7, 1996

Abstract. We present practical approaches for symmetry-adapting valence bond wave functions, with emphasis on the CASVB method. Significant savings in the computational effort become available, both in relation to the application of the Hamiltonian operator and to the reduced number of variational parameters. Results are presented for modern VB representations of CASSCF descriptions of benzene and diborane.

Key words: CASVB – CASSCF – VB – Symmetry adaptation – Spin-coupled

1 Introduction

Although it is standard to make use of molecular point group symmetry in modern computational codes based on molecular orbital theory, the same cannot be said of valence bond calculations that involve the optimization of nonorthogonal orbitals. Existing schemes for making use of symmetry typically require the use of constrained optimization procedures (cf. Ref. [1]); these do not generally lead to any reduction in the computational effort. In this paper we consider some of the issues related to symmetry-adapting VB wave functions, and we propose practical strategies in the context of our CASVB approach [2–4].

After a brief review of the CASVB method in Sect. 2, we discuss in Sect. 3 the symmetry adaptation of VB wave functions. We then examine, in Sect. 4, modern VB descriptions of CASSCF solutions for two highly symmetric systems – benzene and diborane. Both examples are of particular interest in this context, because some CASVB solutions show a tendency to break symmetry. Finally, we present our conclusions in Sect. 5.

* *Current address*: Department of Chemistry, Chemistry Laboratory IV, Copenhagen University, Universitetsparken 5, 2100 Copenhagen ø, Denmark

2 The CASVB approach

Only the main aspects of the CASVB method [2–4] will be outlined here, so as to establish the basic definitions and some notation. The approach, which relies on the invariance of full CI wave functions to general (non-unitary) transformations of the orbitals, has been made available as part of the quantum chemistry package MOLPRO [5], in which it is interfaced to an efficient complete active-space self-consistent field (CASSCF) program [6]. The current implementation allows not only for general modern VB interpretations of CASSCF wave functions, but also for fully variational calculations, including the optimization of core orbitals, and improved capabilities for analyzing the resulting wave function, such as the calculation of derivatives with respect to nuclear displacements. There is little in the way of incorporating the CASVB strategy into other packages which feature CASSCF codes.

We consider a full CI expansion with structures written in the form

$$\Phi_I = \mathscr{A}(\Phi^{\text{core}} \times \Phi_I^{\text{act}}), \tag{1}$$

where Φ^{core} describes the N_{core} "core" electrons, typically using $\frac{1}{2}N_{\text{core}}$ doubly occupied orbitals. The Φ_I^{act} describe the N "active electrons" and they are constructed by allowing all possible occupations of the N active electrons in a set of m active orbitals, compatible with total spin S. We have demonstrated previously [4] the many advantages associated with using simple Slater determinants, but our approach could be applied equally well to spin-adapted configuration state functions (CSFs). On the other hand, it is not useful for CASVB calculations to restrict oneself to *symmetry*-adapted functions for spanning the full-CI space.

A general $m \times m$ orbital transformation $\boldsymbol{O}$ induces and $N_{\text{CI}} \times N_{\text{CI}}$ transformation $\boldsymbol{T}(\boldsymbol{O})$ in the structure space, i.e.

$$\{\phi'\} = \{\phi\}\boldsymbol{O} \Rightarrow \{\Phi'\} = \{\Phi\}\boldsymbol{T}(\boldsymbol{O}), \tag{2}$$

where the $\{\ \}$ denoted row-vectors of the orbitals, ϕ, or many-electron functions, Φ. The effect of $\boldsymbol{T}(\boldsymbol{O})$ can be realized in a very efficient manner by writing $\boldsymbol{O}$ as the product of m^2 simple updates of the form

$$\boldsymbol{O}_{\mu\nu}(\lambda): \phi_\nu \rightarrow \phi_\nu + \lambda\phi_\mu. \tag{3}$$

This can be achieved, for example, by an LU decomposition of $\boldsymbol{O}$, and the corresponding transformation of the many-electron space is then simply realized by successive applications of the excitation operators

$$(\hat{I} + \lambda\hat{E}^{\alpha}_{\mu\nu})\,(\hat{I} + \lambda\hat{E}^{\beta}_{\mu\nu}) = \hat{I} + \lambda\hat{E}^{(1)}_{\mu\nu} + \lambda^2\hat{E}^{(2)}_{\mu\nu}, \tag{4}$$

without explicit construction of $\boldsymbol{T}(\boldsymbol{O})$ [4, 7].

The efficient realization of the structure transformation, Eq. (2), is central to the CASVB approach. As discussed elsewhere [2–4] it can be used for the optimization of VB wave functions, either independently or as a means of generating valence bond interpretations of CASSCF wave functions. In order to achieve this, we express the VB function to be optimized as a linear combination of transformed structures

$$\Psi_{\text{VB}} = \sum_I c_I \mathscr{A}(\Phi^{\text{core}} \times \Phi_I^{\text{VB}}), \tag{5}$$

in which the $\{\Phi^{\text{VB}}\}$ are defined in terms of the nonorthogonal orbital set $\{\phi^{\text{VB}}\}$, constructed by transforming the original full CI space (with orthogonal orbitals). The number of non-zero structure coefficients, c_I, will usually be much

smaller than the dimension of the full CI space, so that such an expansion can be made very compact without sacrificing much of the quality of the wave function. These c_I may of course be optimized freely, but one may wish to put some constraints on them so as, for example, to ensure correct symmetry of the overall wave function.

For generating modern valence bond representations of CASSCF wave functions it is useful to consider two basic families of criteria for optimizing Ψ_{VB}. In the first, we maximize the overlap with a previously optimized CASSCF wave function:

$$S_{\mathrm{VB}} = \frac{\langle \Psi_{\mathrm{CAS}} | \Psi_{\mathrm{VB}} \rangle}{\langle \Psi_{\mathrm{VB}} | \Psi_{\mathrm{VB}} \rangle^{1/2}}. \tag{6}$$

Very high values of S_{VB} may typically be achieved, such that on the order of 99% of the CASSCF wave function may be expressed in simple VB form. In the second criterion, which may be useful for CASSCF wave functions for the lowest state of a given symmetry, we minimize the expectation value for the energy

$$E_{\mathrm{VB}} = \frac{\langle \Psi_{\mathrm{VB}} | \hat{H} | \Psi_{\mathrm{VB}} \rangle}{\langle \Psi_{\mathrm{VB}} | \Psi_{\mathrm{VB}} \rangle}. \tag{7}$$

In both cases, the quantities are optimized with respect to the orbital parameters defining the transformation $\boldsymbol{O}$ from $\{\phi^{\mathrm{CAS}}\}$ to $\{\phi^{\mathrm{VB}}\}$. We may choose to treat the structure coefficients in Eq. (5) as further free parameters. Alternatively, they could be extracted directly from the (transformed) CI vector according to

$$c_{\mathrm{VB}} = \boldsymbol{P}_{\mathrm{VB}} \boldsymbol{T}(\boldsymbol{O}^{-1}) c_{\mathrm{CAS}}, \tag{8}$$

in which $\boldsymbol{P}_{\mathrm{VB}}$ sets to zero the unwanted structure coefficients. These considerations lead to four distinct optimization criteria that we will investigate here:

CASVB1: Maximize S_{VB} with respect to $\boldsymbol{O}$ and structure coefficients.
CASVB2: Maximize S_{VB} with respect to $\boldsymbol{O}$, extracting c_{VB} from the transformed CASSCF CI vector as in Eq. (8).
CASVB3: Minimize E_{VB} with respect to $\boldsymbol{O}$ and structure coefficients.
CASVB4: Minimize E_{VB} with respect to $\boldsymbol{O}$, extracting c_{VB} from the transformed CASSCF CI vector as in Eq. (8),

In the present work we consider mostly the case in which the active part of Ψ_{VB} is built from a single spatial configuration of N singly occupied orbitals, as in spin-coupled theory [8]:

$$\Psi_{\mathrm{VB}} = \mathscr{A}(\Phi^{\mathrm{core}} \phi_1 \phi_2 \ldots \phi_N \Theta^N_{SM}). \tag{9}$$

The N-electron spin function Θ^N_{SM} may be expressed in, and transformed between, various convenient spin bases, the most commonly used being those of Kotani, Rumer and Serber [9]. For Ψ_{VB} of this form, $\boldsymbol{P}_{\mathrm{VB}}$ (Eq. (8)) sets to zero the c_I for all structures in which an active orbital is doubly occupied (the so-called "ionic structures").

3 Symmetry adaptation of VB wave functions

We address in this section the problem of ensuring the correct symmetry of VB wave functions. Symmetry breaking may occur in all areas of *ab initio* quantum chemistry, but in VB theory it raises problems that are quite distinct from those that arise in the majority of MO-based methods. We discuss here two different

approaches that we believe will be the most useful in practical calculations. Ensuring correct symmetry is not only important from the point of view of obtaining a realistic wave function, but the possible associated reduction in computational effort may be of great importance.

The molecular point group $\mathfrak{G}$, of order g, comprises all transformations $\hat{R}$ of the nuclear coordinates that commute with the electronic Hamiltonian. We require trial wave functions to form bases for irreducible representations, $\Gamma^{(i)}$ (dimension d_i), of $\mathfrak{G}$:

$$\hat{R}\{\Psi_1, \ldots, \Psi_{d_i}\} = \{\Psi_1, \ldots, \Psi_{d_i}\}\boldsymbol{D}^{(i)}(R) \quad \forall R \in \mathfrak{G}. \tag{10}$$

Of course, for the important special case in which Ψ is real and $d_i = 1$, this reduces to

$$\hat{R}\Psi = \chi^{(i)}(R)\Psi \quad \forall R \in \mathfrak{G}, \tag{11}$$

with characters $\chi^{(i)}(R) = \pm 1$.

Perhaps the conceptually simplest and most general way of ensuring that a wave function has the correct symmetry is by use of the projection operator

$$\hat{P}^{(i)} = (d_i/g)\sum_R \chi^{(i)}(R)^* \hat{R}. \tag{12}$$

This is a standard group-theoretical result (see, for example, Ref. [10]). The advantage of adopting a projection operator approach is that Eq. (12) may be applied to a wave function of *any* form to ensure a symmetry-pure result. We note that a VB wave function constructed in this way will, in general, be multiconfigurational, and the defining orbitals may be grouped into sets related by symmetry.

The direct symmetry adaptation of combinations of VB structures presents several difficulties, the main reason being that an orbital generated as $\hat{R}\phi_\mu$ will not in general belong to the defining set $\{\phi\}$. An attractive alternative is therefore to apply $\hat{P}^{(i)}$ in the MO basis, in conjunction with two structure transformations, i.e.

$$\boldsymbol{c}_{\mathrm{VB}}^{(i)} = \boldsymbol{T}(\boldsymbol{O}^{-1})\boldsymbol{P}_{\mathrm{MO}}^{(i)}\boldsymbol{T}(\boldsymbol{O})\boldsymbol{c}_{\mathrm{VB}}. \tag{13}$$

Here $\boldsymbol{c}_{\mathrm{VB}}^{(i)}$ is the CI vector in the basis of VB structures, projected such that it transforms as the irreducible representation $\Gamma^{(i)}$. The practicality of such an approach relies on the fact that ensuring the correct symmetry for an MO CI vector is a relatively trivial matter, particularly if only Abelian groups are considered. Each individual MO can be assumed, without loss of generality, to belong to an irreducible representation, and the symmetry of the total spatial configuration can be determined by a simple multiplication of the characters for the orbitals. Applying the projection operator in Eq. (12) then reduces to setting to zero the coefficients for all CSFs (or determinants) that belong to unwanted irreducible representations.

Because the CASVB approach involves expressing Ψ_{VB} in terms of structures formed from orthogonal molecular orbitals (the transformation given in Eq. (13)), it is relatively straightforward to implement the strategy outlined above. The symmetry projection may then be applied after the optimization procedure is completed, so as to remedy a solution that may be symmetry-broken. Alternatively, it may be applied *during* the optimization procedure simply by substituting

$$\Psi_{\mathrm{VB}}^{(i)} = \hat{P}^{(i)}\Psi_{\mathrm{VB}} \tag{14}$$

for Ψ_{VB} in Eqs. (6) and (7). This would then give the optimal symmetry-pure wave function. Both of these alternatives will be considered in Sects. 4 and 5.

We turn now to a second approach for ensuring the correct overall symmetry: the introduction of constraints on the form of the wave function. It is convenient to retain a projection operator formalism, and the condition on the VB wave function

is then that it must be invariant under $\hat{P}^{(i)}$. Furthermore, we will assume here that it is expanded in only a very restricted number of spatial configurations. It is well known that the complete set of spin eigenfunctions for N electrons always form a basis for the permutation group $\mathscr{S}_N$. This leads to the finding, as has been discussed in detail by Gerratt [11], that the most generally applicable way of ensuring the correct overall symmetry is to require that the operations $\hat{R}$ induce only *permutations* of the defining orbital set:

$$\hat{R}\phi_\mu = \zeta_{\mu\nu}(R)\phi_\nu \quad \forall R \in \mathfrak{G}, \tag{15}$$

where $\zeta_{\mu\nu}(R) = \pm 1$ for real orbitals. In practice, it is sufficient to satisfy Eq. (15) for the *generators* of $\mathfrak{G}$.

Ensuring fulfilment of the orbital conditions, Eq. (15), is usually quite straightforward. The only orbital parameters retained in the optimization procedure are those associated with the symmetry-unique orbitals, which generate the full $\{\phi^{\mathrm{VB}}\}$ by successive applications of the group operators. The remaining parameters may be eliminated by standard procedures. If a symmetry-unique orbital is not permuted by a symmetry operator, i.e.

$$\hat{R}\phi_\mu = \zeta_{\mu\mu}(R)\phi_\mu, \tag{16}$$

then the matrix representation of $\hat{R}$ (which in general is non-symmetric) can be diagonalized, and ϕ_μ expanded in only the real, right-hand eigenvectors which have the eigenvalue $\zeta_{\mu\mu}(R)$. The number of free parameters associated with variations of this orbital will then be $N_{\mathrm{eig}} - 1$, where N_{eig} is the number of acceptable eigenvectors and the normalization condition imposes one further constraint.

Besides the orbital conditions set out in Eq. (15), we must also put the following simple requirements on the structures defining the wave function:

1. The list of spatial configurations must be closed under the permutations induced by the symmetry operators. For example, if $\hat{\sigma}_v$ induces the interchange $1 \leftrightarrow 2$, then the configuration 11 2 3 implies also the configuration 22 1 3.
2. If $\boldsymbol{R}$ is the matrix representation of $\hat{R}$ in the structure basis,[1] then the structure coefficients must be formed as a linear combination of real right-hand eigenvectors of this matrix with eigenvalues $\chi^{(i)}(R)$ (as defined in Eq. (11)).

It is again sufficient to consider only the *generators* of the point group.

We have in this way two very different strategies, either of which may be used to ensure a symmetry-pure wave function during the optimization procedure. They may also be applied in combination: constraints could be used that are appropriate to a subgroup of the full molecular point group or that relate only to a subset of orbitals, and the projection operator then applied to ensure correct symmetry of the final wave function. We shall investigate various possibilities in Sects. 4 and 5.

4 Results

The calculations described in this section were all carried out using the CASSCF [6] and CASVB [3, 4] modules in MOLPRO [5], or with our own spin-coupled code [12].

[1] The existence of this matrix representation is ensured by the fulfilment of requirement 1, combined with the fact that $\hat{R}$ induces a simple permutation of the orbital set.

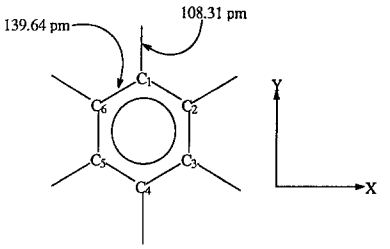

Fig. 1. The geometry, orientation, and atom numbering adopted for benzene

Table 1. Energies for benzene. Details of the various calculations are given in the text

Calculation	E[hartree]	$(E - E_{CAS})$ [millihartree]
SCF	−230.764056	72.77
SC^{CAS}	−230.829233	7.59
SC	−230.829331	7.49
SC + CI	−230.836729	0.09
CASSCF	−230.836822	(0)

4.1 Benzene

The geometry, orientation, and atom numbering adopted for C_6H_6 (D_{6h} symmetry) are as shown in Fig. 1. For C/H we used correlation consistent pVTZ basis sets [13], (10*s*5*p*2*d*/5*s*2*p*) contracted to [4*s*3*p*2*d*/3*s*2*p*], but in order to limit the size of the problem, the polarization functions were replaced with just a single Cartesian *d* Gaussian on carbon with $\alpha = 0.8$, and a single *p* Gaussian on each hydrogen with $\alpha = 1.0$.

A "6 in 6" CASSCF calculation was performed for the π electrons, keeping the 36 σ electrons in an (optimized) closed-shell core. The correlation energy retrieved by this wavefunction amounts to 72.8 millihartree (see Table 1). The natural orbitals for the π system resemble the MOs in the well-known SCF picture; in order of decreasing occupation numbers they are: $1a_{1u}$, two components of $1e_{1g}$, two components of $1e_{2u}$, and $1b_{1g}$. The CASSCF calculations were actually carried out in the Abelian subgroup D_{2h}, in which the active MOs φ_1–φ_6 can be classified as $1b_{1u}$ (transforming as Z), $1b_{2g}(XZ)$, $1b_{3g}(YZ)$, $1a_u(XYZ)$, $2b_{1u}(Z)$ and $2b_{3g}(YZ)$.

The spin-coupled (SC) description of benzene has been reported previously in several publications [14]. In the present calculation, the SC orbitals were expanded in all functions of π symmetry, *i.e.* those which are antisymmetric with respect to reflection in the molecular plane. For ease of comparison, the core orbitals for the SC wave function were taken from the CASSCF calculation, without further optimization. The SC solution thus obtained consists of six singly occupied, nonorthogonal orbitals, equivalent by successive $\hat{C}_6$ rotations (see Fig. 2). These orbitals are essentially localized $C(2p_\pi)$ functions, but they exhibit some delocalization towards the neighbouring carbon atoms in the ring. It is useful to label these orbitals according to the carbon atoms with which they are associated. The coupling of the associated electron spins is conveniently expressed in the Rumer basis. Rumer functions 1 and 4 correspond to Kekulé structures whereas the others

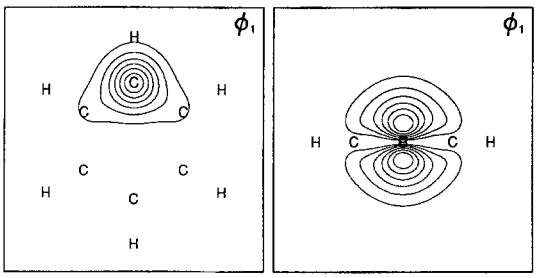

Fig. 2. Symmetry-unique SC orbital for benzene. Orbital contours are plotted in the plane $Z = 1$ bohr (left), and in the plane parallel to $Y = 0$ and containing C1 (right)

Table 2. Weights of the Rumer spin functions in the total spin function for the various orbital sets in benzene

	Θ_{K1}	Θ_{K2}	Θ_{D1}	Θ_{D2}	Θ_{D3}
SC	40.60%	40.60%	6.27%	6.27%	6.27%
CASVB1	36.53%	36.53%	8.98%	8.98%	8.98%
CASVB2	32.92%	32.92%	11.48%	11.33%	11.33%
CASVB2 (s)	32.37%	32.37%	11.75%	11.75%	11.75%
CASVB3	40.62%	40.62%	6.26%	6.26%	6.26%
CASVB4	32.09%	33.57%	11.48%	11.38%	11.48%
CASVB4 (s)	32.56%	32.56%	11.63%	11.63%	11.63%
CASVB1 (E)	40.96%	40.96%	6.03%	6.03%	6.03%
CASVB1 (C)	31.37%	31.37%	12.42%	12.42%	12.42%

Note: (s) signifies symmetry-constrained solutions. CASVB1 (E) and CASVB1 (C) are the energy-optimized and CASSCF spin-coupling coefficients, respectively, based on the CASVB1 orbital set

(functions 2, 3 and 5) correspond to para-bonded or Dewar structures. The Kekulé structures dominate the total wave function (see Table 2): these two spin functions each have Chirgwin–Coulson weights (ω) of 40.6%.

About 0.0022% of each SC orbital was found to lie outside the CASSCF active space, i.e. to be expanded in virtual CASSCF MOs. This relatively low value is likely to be associated with the reduced number of free parameters arising from the high symmetry of benzene, and it is reflected in the energy differences seen in Table 1. Augmenting the spin-coupled wave function with all possible ionic structures within the active space ("SC + CI") gives a wave function within 0.09 millihartree of the CASSCF value. This difference can be attributed solely to the difference between the active spaces. Likewise, performing a spin-coupled calculation using only the active CASSCF MOs as expansion functions ("SC^{CAS}") leads to an energy 0.1 millihartree higher than the SC energy. The energy differences related to the difference in the active spaces are thus of a similar order of magnitude. They are much smaller than the difference associated with the exclusion of ionic structures (about 7.5 millihartree).

We now turn to the modern VB interpretations of the CASSCF wave function. For all four CASVB criteria, the SC picture was reproduced extraordinarily well, as may be seen from Fig. 3. CASVB2 and CASVB4 have been constrained here to have the correct symmetry, as discussed later. The overlap integrals (see Table 3) are a more sensitive indication of orbital change than the figures, and some variation between the sets may be discerned. However, the variations in the spin-coupling coefficients listed in Table 2 are mostly related to the mode of

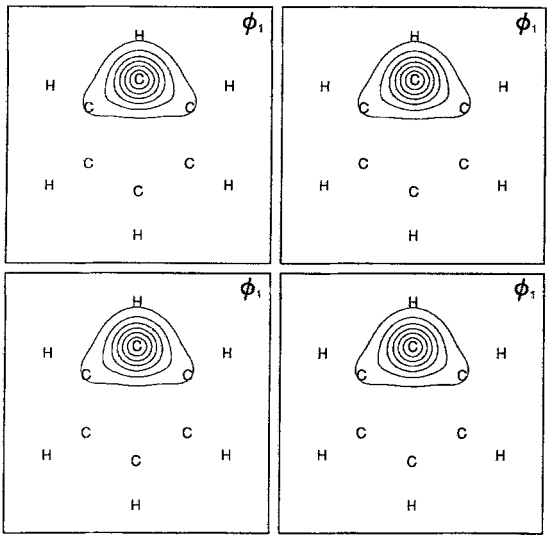

Fig. 3. Symmetry-unique benzene orbitals for the symmetric CASVB1-CASVB4 solutions, plotted in the plane $Z = 1$ bohr

Table 3. Symmetry-unique overlap integrals for the symmetric orbitals sets in benzene

	$\langle\phi_1/\phi_2\rangle$	$\langle\phi_1/\phi_3\rangle$	$\langle\phi_1/\phi_4\rangle$
SC	0.52383	0.02939	− 0.15700
CASVB1	0.51564	− 0.01664	− 0.21672
CASVB2 (s)	0.49919	− 0.07186	− 0.27225
CASVB3	0.52355	0.02809	− 0.15804
CASVB4 (s)	0.50056	− 0.04674	− 0.23127

structure coefficient optimization, rather than the differences between the orbital sets. This can be seen from the spin-coupling coefficients for the CASVB1 orbital set, which were calculated by maximizing S_{VB} (first entry in Table 2), minimizing E_{VB} (CASVB1 (E)), or by projecting the CASSCF wave function (CASVB1 (C)). The general trend of the weights for the Kekulé structures,

$$\omega(\Theta_{KI})(E) > \omega(\Theta_{KI})(S) > \omega(\Theta_{KI})(C), \tag{17}$$

was observed for all the orbital sets [2]. This is consistent with the trends in the nearest-neighbour overlaps reported in Table 3, as a higher degree of singlet coupling is generally associated with larger overlaps.

The main difference from the SC description was a marked propensity for symmetry-breaking in the case of CASVB2 and CASVB4. The two orbital sets are shown in Figs. 4 and 5. It should be noted that both solutions retain some degree of symmetry, in the form of σ_v mirror planes; for CASVB2, this plane contains two opposite carbon atoms (C1 and C4 in Fig. 4) whereas for CASVB4 it bisects two bonds (C1–C2 and C4–C5 in Fig. 5). This is most easily verified by examining the overlap integrals (Table 4) and the spin-coupling coefficients (Table 2). Both criteria extract the spin-coupling coefficients from the transformed CASSCF wave function, and it therefore seems most likely that the symmetry-breaking is related to the reduced number of degrees of freedom when the spin coupling is constrained in this manner.

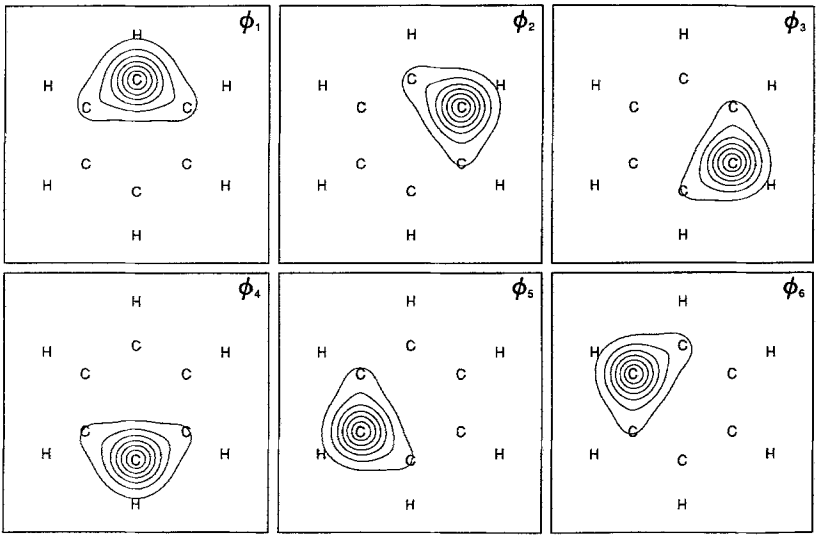

Fig. 4. CASVB2 orbitals of benzene, plotted in the plane $Z = 1$ bohr

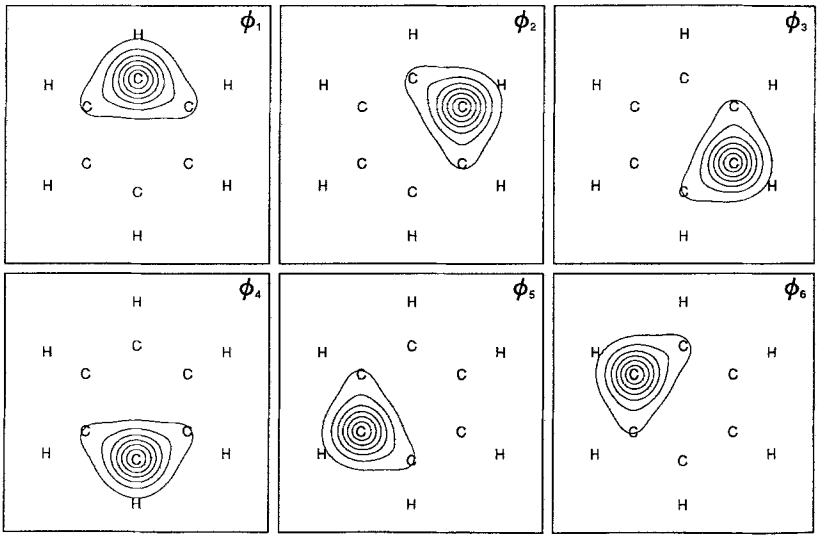

Fig. 5. CASVB4 orbitals of benzene, plotted in the plane $Z = 1$ bohr

We now examine procedures for symmetry-adapting these solutions. In order to ensure the correct overall symmetry by means of constraints, it is sufficient to consider the generating symmetry operations $\hat{\sigma}_X$ (reflection plane $X = 0$) and $\hat{C}_6$. The analogous conditions associated with the $\hat{\sigma}_z$ reflection are of course fulfilled implicitly, because of the π symmetry of the active MOs.

We consider first the condition on ϕ_1, namely that it must be invariant under the $\hat{\sigma}_X$ reflection:

$$\hat{\sigma}_X \phi_1 = \phi_1. \tag{18}$$

Table 4. Overlap matrices for the non-symmetric orbital sets in benzene

CASVB2	1	2	3	4	5	6
1	1	0.58673	0.05608	−0.24512	0.05608	0.58673
2		1	0.48906	−0.18195	−0.24708	0.16706
3			1	0.42168	−0.24581	−0.24708
4				1	0.42168	−0.18195
5					1	0.48906
6						1
CASVB4						
1	1	0.56136	0.09910	−0.21989	−0.04748	0.54559
2		1	0.54559	−0.04749	−0.21989	0.09911
3			1	0.44734	−0.16611	−0.21464
4				1	0.45757	−0.16611
5					1	0.44734
6						1

The matrix representation of $\hat{\sigma}_X$ is already diagonal in the MO basis, with diagonal elements 1, −1, 1, −1, 1 and 1, and so Eq. (18) can be fulfilled simply by expanding ϕ_1 only in MOs φ_1, φ_3, φ_5 and φ_6.

The matrix representation of $\hat{C}_6$ is more complicated since only MOs φ_1 and φ_6 form one-dimensional representations (with characters +1 and −1 respectively). The remaining MOs form two two-dimensional bases, which may be expressed

$$\hat{C}_6\{\varphi_2, \varphi_3\} = \{\varphi_2, \varphi_3\}\begin{pmatrix} \frac{1}{2} & -\frac{1}{2}\sqrt{3} \\ \frac{1}{2}\sqrt{3} & \frac{1}{2} \end{pmatrix} \tag{19}$$

and

$$\hat{C}_6\{\varphi_4, \varphi_5\} = \{\varphi_4, \varphi_5\}\begin{pmatrix} -\frac{1}{2} & -\frac{1}{2}\sqrt{3} \\ \frac{1}{2}\sqrt{3} & -\frac{1}{2} \end{pmatrix}. \tag{20}$$

Each of these matrix representations is orthogonal, because $\hat{C}_6^6 = \hat{I}$, and the traces correspond to the characters of E_{1g} and E_{2u} in D_{6h}. The signs of the off-diagonal elements depend on the (arbitrary) relative phases of the MOs, and so some care is required when repeating calculations to ensure consistent phases. Having constructed the full matrix representation of $\hat{C}_6$ in this manner, it is then trivial to construct he remaining orbitals by successive rotations, if $\boldsymbol{O}^{(i)}$ refers to the ith column of the orbital transformation matrix, i.e. the expansion of CASVB orbital ϕ_i in the active MOs, then

$$\boldsymbol{O}^{(i)} = \boldsymbol{C}_6^{(i-1)}\boldsymbol{O}^{(1)}. \tag{21}$$

The structure coefficients may be constrained by considering the orbital permutations induced by the $\hat{C}_6$ rotation: (234561), and the $\hat{\sigma}_X$ reflection: (165432). In the case of a Ψ_{VB} of SC form, this can be achieved by constructing the spin function representation matrices for the inverse permutations of electron labels, diagonalizing them, and extracting the eigenvectors with eigenvalues $\chi^{(i)}$ (+1 in this case). To satisfy both conditions we simply take the intersection of these two vector spaces. In this way, we obtain two linearly independent symmetry-adapted spin functions,

Table 5. Values of S_{VB} and E_{VB} for the various orbital sets in benzene. (s) signifies symmetry-constrained solutions, (p) the symmetry-projected values, and (P) the values where the symmetry-projected wave function was optimized (see text)

	S_{VB}	E_{VB}
CASVB1	0.99546	−230.828917
CASVB2	0.99545	−230.828792
CASVB2 (s)	0.99543	−230.828776
CASVB2 (p)	0.99564	−230.829106
CASVB3	0.99517	−230.829233
CASVB4	0.99517	−230.829060
CASVB4 (s)	0.99515	−230.829051
CASVB4 (p)	0.99529	−230.829241
CASVB1 (P)	$1-(8\times10^{-6})$	−230.836796
CASVB2 (P)	0.99996	−230.836699
CASVB3 (P)	$1-(8\times10^{-6})$	−230.836796
CASVB4 (P)	0.99996	−230.836702

most conveniently expressed in the Rumer basis:

$$\Theta_a = \Theta_{K1} + \Theta_{K2} \tag{22}$$

and

$$\Theta_b = \Theta_{D1} + \Theta_{D2} + \Theta_{D3}. \tag{23}$$

This outcome is of course intuitively obvious, but more complicated cases will require diagonalization of the structure representation matrix.

Incorporating symmetry constraints thus leads to a vastly simplified problem, in which the number of variational parameters is reduced from 34 to only 4 for CASVB1 and CASVB3, and from 30 to 3 for CASVB2 and CASVB4. The results for CASVB2 and CASVB4 are illustrated in Fig. 3, with numerical values in Tables 2 and 3. A further point to note is the extent of the reduction in quality of the constrained wave functions, as measured by the decrease of S_{VB} or increase in E_{VB} (see Table 5). The symmetry-pure CASVB2 wave function is just 2×10^{-5} lower in its overlap with the CASSCF wave function and CASVB4 just 9 microhartree higher in energy. The small sacrifice in accuracy is clearly more than outweighed by the increased simplicity of the solution.

To shed further light on the nature of the symmetry breaking, the *full* Hessians for the converged symmetry-pure solutions were examined. For each CASVB criterion, there were two very small eigenvalues relating to variations in the orbital parameters. In some cases these were positive and in others negative, rendering the symmetry-pure solutions unstable. The symmetry breaking in certain unconstrained CASVB descriptions of benzene may thus seem somewhat accidental in nature. We note, however, that these features were reproduced with several different basis sets. Changing the basis set did affect slightly the proportion of each SC orbital which lies outside the CASSCF active space.

We turn now to the projection operator defined in Eq. (12). Transforming to the CASSCF MO basis and setting to zero coefficients of determinants not belonging to the A_g irreducible representation in D_{2h} seems sufficient for practical purposes, and demonstrates the basic features of the approach. We first consider the

Table 6. Energies for diborane. Details of the various calculations are given in the text

Calculation	E[hartree]	$(E - E_{CAS})$ [millihartree]
SCF	−52.815220	90.32
SC	−52.893038	12.51
CAS B	−52.898012	7.53
CAS A	−52.905543	(0)

symmetry adaptation of symmetry-broken solutions without further optimization. Since the projection operator annihilates only parts of the orthogonal complement of the CASSCF CI vector, we must have $S_{VB}^{(s)} \geqslant S_{VB}$. For the same reason, symmetry projection is likely to lead to a lowering in energy, although exceptions from this rule may occur. It is somewhat surprising that the S_{VB} and E_{VB} values for the symmetrized CASVB2 and CASVB4 wave functions (see Table 5) surpass the optimal single configuration results (CASVB1 and CASVB3).

Of course, symmetrization of the CASVB1 and CASVB3 solutions has no effect, since these wave functions already have the required symmetry. However, as seen above, allowing distortion away from the correct symmetry can lead to better values for S_{VB} and E_{VB}. Indeed, very impressive values could be obtained in free optimization of the projected wave functions (see Table 5): this can be seen as a consequence of restoring the number of variational parameters from 4 to 34 (CASVB1 and CASVB3) or from 3 to 30 (CASVB2 and CASVB4). As may be expected, the orbitals are heavily distorted and the interpretation of the wave functions becomes significantly more complex. As such, a full optimization incorporating the projection operator is not to be recommended.

4.2 Diborane

For B_2H_6 (D_{2h} symmetry) we used $r_{BB} = 176.65$ pm, $r_{BH^t} = 120$ pm, $r_{BH^b} = 132.6$ pm and $\angle(B\text{–}B\text{–}H^t) = 121°$, where H^t and H^b refer to the terminal and bridging hydrogen atoms, respectively. For B/H we employed correlation consistent pVDZ basis sets [13] consisting of (9*s*4*p*1*d*/4*s*1*p*) Cartesian Gaussian functions contracted to [3*s*2*p*1*d*/2*s*1*p*].

Four electrons were accommodated in (optimized) core orbitals, corresponding essentially to the $1s^2$ on both boron atoms, leaving 12 valence electrons to be described by a "12 in 12" CASSCF expansion. The lowest solution thus found, which we denote "CAS A", retrieves 90.32 millihartree of correlation energy (see Table 6). In addition, we also investigated a second solution, "CAS B", lying 7.5 millihartree higher in energy.

A 12-electron SC calculation, incorporating all 132 allowed modes of spin coupling, was carried out with Φ^{core} taken directly from the CASSCF wave function. The SC description reproduces the findings obtained with lower levels of theory: these include SOPP-GVB calculations [15] and earlier SC treatments [16]. The B–H^t bonds are described by B(sp^x-type) hybrids overlapping essentially 1*s* orbitals on H (see Fig. 6). The corresponding electron spins are to a good approximation singlet coupled. Each of the 3-center-2-electron bonds in the bridging region is best described as follows. One of the orbitals is a deformed 1*s* function

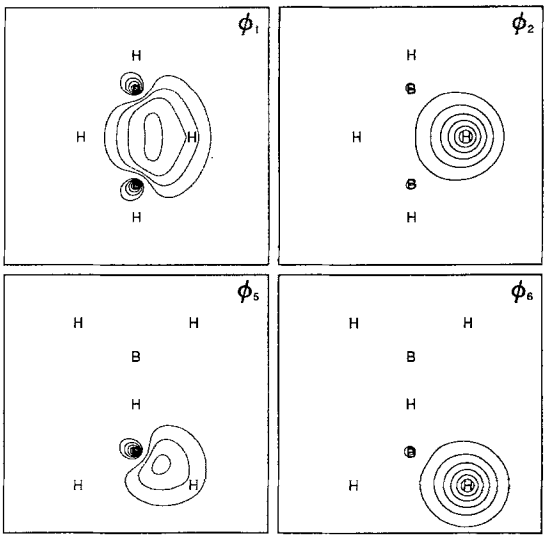

Fig. 6. Symmetry-unique spin-coupled orbitals for diborane

on H^b. The other consists of *two* "fused" B(sp^x-type) hybrids pointing towards the H^b (see Fig. 6). Again the corresponding electron spins are predominantly singlet coupled, such that the overall weight of the perfect-pairing spin function is 95.58%.

A rather different picture for the bridging region emerges from the CASVB interpretations of the "CAS A" solution. We now see a distinctly two-center description (see Fig. 7), arising from somewhat deformed B (sp^x-type) hybrids delocalized onto the H^b atoms. There are no orbitals associated solely with the hydrogen. Furthermore, there is significant symmetry-breaking. The description of the B–H^t bonds is virtually unchanged from that provided by the SC calculation.

A symmetry-pure solution can be obtained from the CASVB wave functions just described if the upper and lower bridging B(sp^x-type) hybrids are made equivalent under the $\hat{\sigma}_z$ reflection. The orbital conditions can then be satisfied by considering the generating group elements $\hat{\sigma}_x$, $\hat{\sigma}_y$ and $\hat{\sigma}_z$. For the structure coefficients, we must diagonalize the structure representation matrices for the three permutations (3 4 1 2 5 6 7 8 9 10 11 12), (1 2 3 4 7 8 5 6 11 12 9 10) and (2 1 4 3 9 10 11 12 5 6 7 8), induced by $\hat{\sigma}_x$, $\hat{\sigma}_y$ and $\hat{\sigma}_z$, respectively. To ensure the simultaneous fulfillment of all three conditions, we take the intersection of the three vector spaces spanned by eigenvectors with eigenvalues $+1$ (cf. the case of benzene). This leads to a reduction in the number of allowed structures from 132 to 32, in addition to the reduction of orbital parameters from 132 to 25.

The constrained bridging orbitals are shown in Fig. 8. The loss of accuracy upon incorporating symmetry constraints was somewhat larger in this case than for benzene: 0.2 millihartree for CASVB1, for example (see Table 7). It is thus no longer so clear-cut that incorporating constraints is a satisfactory solution. An alternative is to allow a multiconfigurational description of the bridging region. We therefore performed a further optimization in which the equivalence between upper and lower bridging orbitals was released, and the projection operator invoked instead. It seems reasonable to retain the equivalence between B–H^t bonds, as well as the left–right equivalence in the bridging region. The resulting orbitals are shown in Fig. 9.

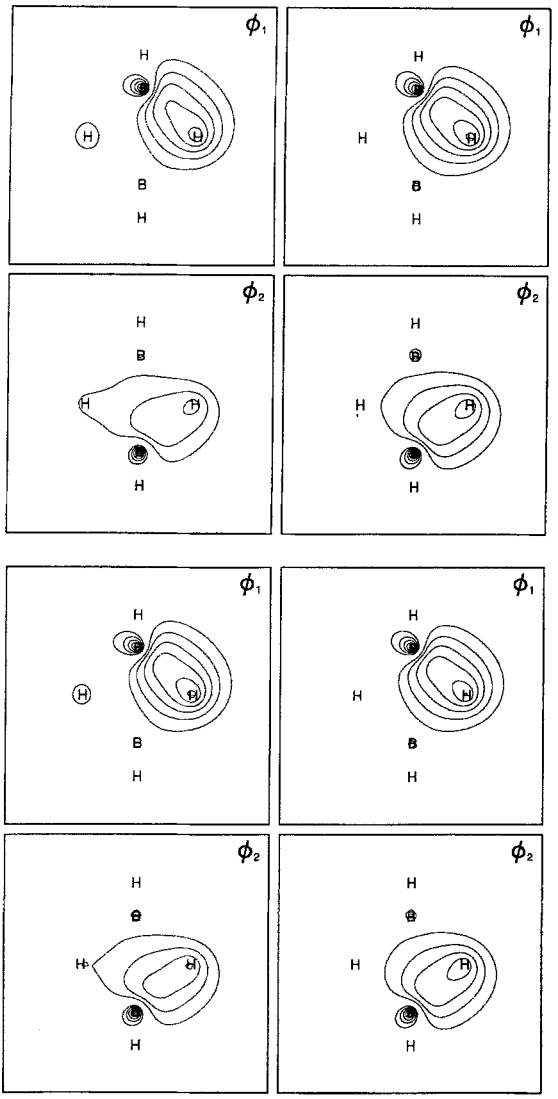

Fig. 7. Bridging region CASVB1–CASVB4 solutions for diborane ("CAS A")

We now address the inconsistency with the spin-coupled solution and, indeed, the description that emerges from applying standard localization procedures to the SCF MOs. Looking at just the orbitals for the bridging region, it is clear that the "CAS A" wave function, and its various CASVB interpretations, transforms as $A_g + B_{2g} + B_{1u} + B_{3u}$ whereas those from the SC calculation transform as $2A_g + 2B_{3u}$. As such, the lowest CASSCF solution is *incompatible* with the traditional SC description of the bridging region. The secondary CASSCF wave function, "CAS B", with the "correct" distribution of active MOs among the irreducible representation lies 7.5 millihartree above the "CAS A" solution. It gives the CASVB representations illustrated in Fig. 10: these are very similar to the standard SC result. Furthermore, the values for S_{VB} and E_{VB} based on "CAS B" (see Table 8) are significantly better than those for the solution lowest in energy. It is clear that the

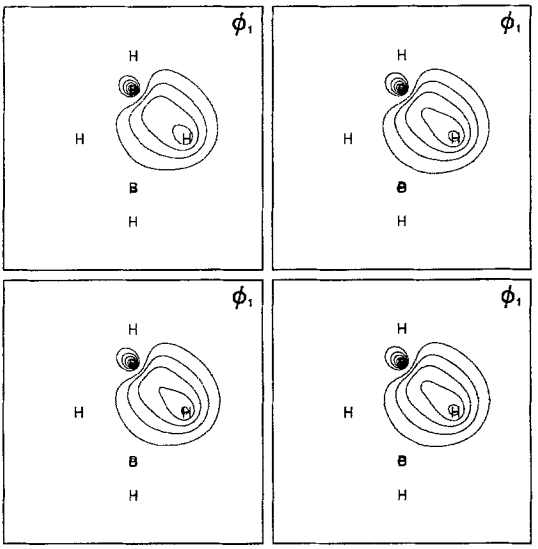

Fig. 8. Symmetric bridging region CASVB1–CASVB4 orbitals for diborane ("CAS A")

Table 7. Values of S_{VB} and E_{VB} for the various orbital sets in diborane ("CAS A")

	S_{VB}	E_{VB}
CASVB1	0.99571	− 52.889322
CASVB2	0.99552	− 52.889201
CASVB3	0.99557	− 52.889782
CASVB4	0.99540	− 52.889496
CASVB1 (s)	0.99549	− 52.889112
CASVB2 (s)	0.99548	− 52.889148
CASVB3 (s)	0.99537	− 52.889443
CASVB4 (s)	0.99535	− 52.889417
CASVB1 (p)	0.99590	− 52.890116
CASVB2 (p)	0.99556	− 52.889389
CASVB3 (p)	0.99569	− 52.890316
CASVB4 (p)	0.99543	− 52.889632
CASVB1 (sP)	0.99606	− 52.890312
CASVB2 (sP)	0.99585	− 52.889674
CASVB3 (sP)	0.99589	− 52.890791
CASVB4 (sP)	0.99572	− 52.889966

Note: (s) signifies the symmetry-constrained solutions, (p) the symmetrized values for the simple solutions, and (sP) the combination of symmetry constraints and projection operator as described in the text

"CAS B" wave function is much better *suited* to a single configuration SC-like interpretation than is "CAS A".

We note that also for "4 in 4" CASSCF treatments, concentrating on the valence electrons associated with the bridging region, solution A lies slightly lower in energy than solution B (−52.840084 hartree and −52.838508 hartree, respectively). CASVB interpretations of these two "4 in 4" wave functions produce the same rival descriptions of the bridging region as described above.

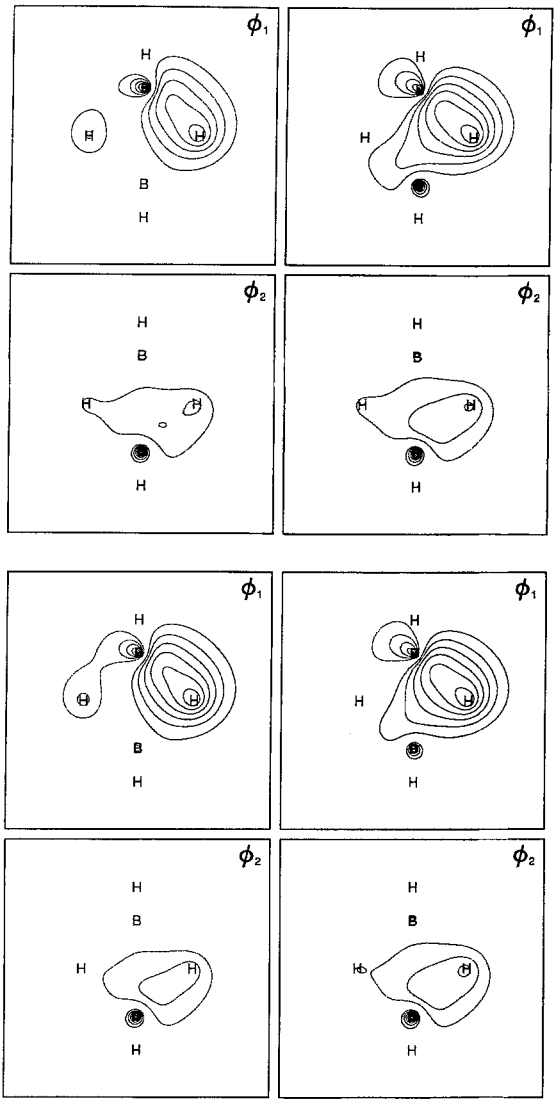

Fig. 9. Bridging CASVB1–CASVB4 solutions for diborane, optimized with the projection operator ("CAS A")

In the systems we have studied so far [2–4] it has always been possible to construct a CASSCF expansion which has CASVB interpretations that are exceedingly similar to the SC picture. However, in the case of diborane, the lowest solution is incompatible with the simple SC picture; it seems necessary to invoke some sort of multiconfigurational description in order to obtain an accurate CASVB representation of this wave function. An alternative is to examine instead the "CAS B" solution, in spite of its slightly higher energy. A situation with two rival CASSCF solutions has also been found for a π-electron treatment of ozone [3], but in that case *both* solutions had straightforward SC analogues. It is interesting to note, however, that when a linear combination of the two SC-like configurations is constructed, it is the one corresponding to the CASSCF with slightly higher energy that dominates the total wave function.

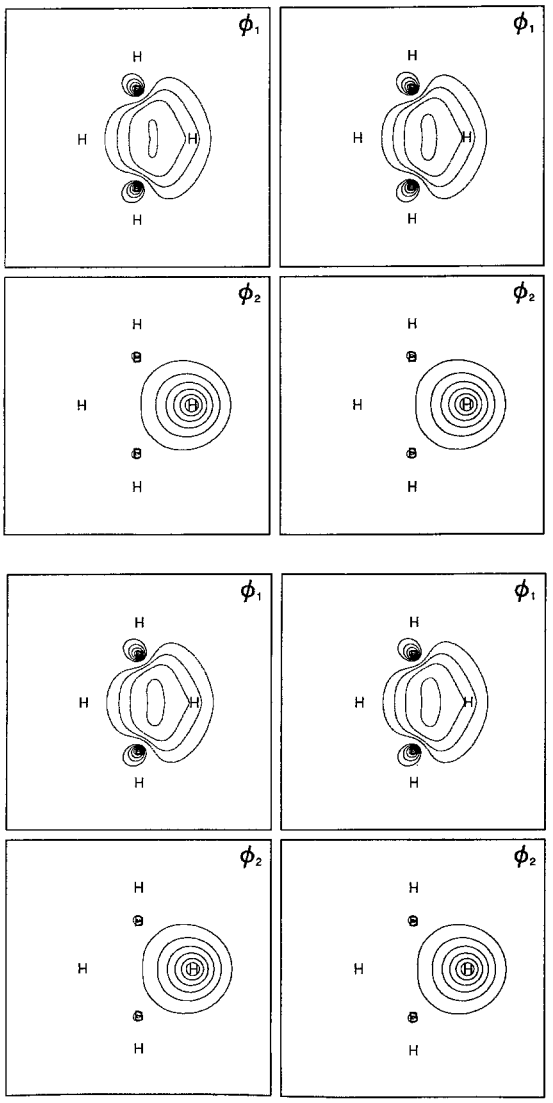

Fig. 10. Bridging region CASVB1–CASVB4 solutions for diborane ("CAS B")

5 Conclusions

It seems useful to distinguish between two separate categories of symmetry breaking: cases with a clear underlying physical reason and the more "accidental" cases. The classification may in each individual case be somewhat subjective, but the differences in S_{VB} and E_{VB} between constrained and symmetry-broken solutions can provide one useful indication. A large increase in E_{VB} upon invoking constraints, for example, would suggest a definite physical reason behind the breaking of symmetry. In the case of diborane it seems reasonable to argue that the symmetry breaking is a consequence of forcing a single configuration description

Table 8. Values of S_{VB} and E_{VB} for the various orbital sets in diborane ("CAS B")

	S_{VB}	E_{VB}
CASVB1	0.99862	− 52.892407
CASVB2	0.99861	− 52.892413
CASVB3	0.99861	− 52.892450
CASVB4	0.99860	− 52.892435

on the electron-deficient bridging region. For benzene on the other hand, the symmetry breaking is clearly more accidental, depending as it does on the precise way in which the optimizations are performed.

It should be emphasized that fully variational SC calculations for benzene and diborane do *not* break symmetry. One reason why the CASVB descriptions of these molecules may exhibit a greater tendency towards symmetry breaking could be the constraints inherent in the choice of CASSCF active space, i.e. in the particular distribution of active MOs among the irreducible representations.

To our knowledge, this work represents the first general use of the symmetry projection operator (Eq. (13)) in VB calculations that involve the optimization of nonorthogonal orbitals. However, a related procedure has been employed for degenerate irreducible representations in SC calculations: the various symmetry-related spatial configurations are each constructed separately and solution of the subsequent secular problem provides eigenvectors with the desired symmetry properties. An example of this approach is the construction of the two degenerate components of E'' for the cyclopropenyl radical [17]. It seems very likely that the resulting solutions will prove to be very similar to those obtained by an application *a posteriori* of the symmetry projection operator.

It is useful to summarize various features of the two approaches that we have outlined here for symmetry adapting CASVB wave functions:

Symmetry constraints:
- Reduces the number of free parameters, and hence reduces the computational effort as well as simplifying the optimization procedure.
- Retains a simple form for the wave function.
- Assumes a particular form of solution.

Projection operator:
- Preserves the number of free parameters. Hence, gives better values for S_{VB} and E_{VB}.
- Generally complicates the form of the wave function.
- Makes no assumptions as to the form of solution.

In the case of "spurious" breaking of symmetry, it seems natural to invoke constraints, whereas in cases with an underlying physical reason, it may be more appropriate to adopt the projection operator approach. However, we cannot recommend indiscriminate use of the projection operator, since results thus obtained, while achieving high accuracy, tend to lose many of the interpretational advantages generally associated with a compact VB description.

As was seen in the examples, introducing constraints can vastly reduce the number of variational parameters. This significantly influences performance, such

that it may be advantageous to invoke constraints even if this is not actually required for convergence to a symmetry-pure solution. This is a consequence of a feature of the CASVB procedure that the computational effort per iteration is approximately proportional to the number of free parameters in the optimization [4]. However, the main problem in applying constraints is that it can be very difficult *a priori* to make a good judgement regarding the form of the solution.

It is worth reiterating the many advantages associated with using an underlying basis of symmetry-adapted orbitals, as we have done here. The projection operator is very simple to invoke in this formalism. Similarly, the orbital constraints take on a very much simpler form than they would do otherwise. Furthermore, diagonalizing the non-symmetric structure representation matrix for orbital permutations induced by the generating group elements seems a very straightforward way of imposing the proper constraints on the structure coefficients.

Applying the Hamiltonian operator to a full-CI vector was first considered by Siegbahn [18], and the most efficient approach [19] is derived from his original algorithm. The reduction in computational effort associated with the utilization of point group symmetry is very significant in this scheme. One may loop over irreducible representations, applying the Hamiltonian operator only if there are non-zero coefficients. Thus, use of symmetry leads to savings even if the CI vector is not symmetry-pure, but there are additional savings if the CI vector can be assumed to belong to a given irreducible representation.

These considerations are, of course, not crucial for CASVB1 or CASVB2, which do not involve the Hamiltonian operator, and which are, in any case, computationally much cheaper than their energy-based counterparts. As such a practical approach seems to be to perform an initial overlap-based optimization as a precursor for a more expensive energy-based calculation (CASVB3 or CASVB4). The form of the overlap-based solution thus obtained will suggest what constraints might be appropriate, and whether a projection operator should be invoked. Support for this strategy comes from our experience that analogous overlap- and energy-optimized wave functions are always in very good qualitative agreement.

We have presented practical approaches for symmetry-adapting valence bond wave functions, with emphasis on the CASVB method. These techniques should prove useful for the proper utilization of molecular point group symmetry in various valence bond approaches that involve the optimization of nonorthogonal orbitals.

References

1. Karadakov PB, Gerratt J, Raimondi M, Cooper DL (1992) J Chem Phys 97:7635
2. Thorsteinsson T (1995) Development of methods in spin-coupled theory. PhD thesis, University of Liverpool, UK
3. Thorsteinsson T, Cooper DL, Gerratt J, Karadakov PB, Raimondi M (1996) Theor Chim Acta 93:343
4. Thorsteinsson T, Cooper DL (1996) Theor Chim Acta 94:233
5. MOLPRO is a package of *ab initio* programs written by Werner H-J, Knowles PJ with contributions from Almlöf J, Amos RD, Berning A, Deegan MJO, Eckert F, Elbert ST, Hampel C, Lindh R, Meyer W, Nicklaß A, Peterson K, Pitzer R, Stone AJ, Taylor PR, Mura ME, Pulay P, Schütz M, Stoll H, Thorsteinsson T, Cooper DL
6. Werner H-J, Knowles PJ (1985) J Chem Phys 82:5053; Knowles PJ, Werner H-J (1985) Chem Phys Lett 115:259
7. Malmqvist PÅ (1986) Int J Quant Chem 30:479

8. For a review of applications see, for example: Cooper DL, Gerratt J, Raimondi M (1991) Chem Rev 91:929
9. Karadakov PB, Gerratt J, Cooper DL, Raimondi M (1995) Theor Chim Acta 90:51
10. Hamermesh G (1962) Group theory and its application to physical problems. Addison-Wesley, Reading, MA, Sect. 3–18
11. Gerratt J (1971) Adv Atom Mol Phys 7:141; See also: Wright SC, Cooper DL, Gerratt J, Raimondi M (1992) J Phys Chem 96:7943
12. Cooper DL, Gerratt J, Raimondi M, Sironi M, Thorsteinsson T (1993) Theor Chim Acta 85:261
13. Dunning TH (1989) J Chem Phys 90:1007
14. Cooper DL, Gerratt J, Raimondi M (1986) Nature 323:699; Cooper DL, Wright SC, Gerratt J, Hyams PA, Raimondi M (1989) J Chem Soc, Perkin Trans 2:719; da Silva EC, Gerratt J, Cooper DL, Raimondi M (1994) J Chem Phys 101:3866
15. Wilson S, Gerratt J (1975) J Mol Phys 30:765
16. Cooper DL, Gerratt J, Raimondi M (1991) J Mol Struc (THEOCHEM) 229:155; Sironi M, Raimondi M, Cooper DL, Gerratt J (1991) J Phys Chem 95:10617
17. Gerratt J, Cooper DL, Raimondi M (1990) In: Klein DJ, Trinastic N (eds) Valence bond theory and Chemical Structure. Elsevier, Amsterdam
18. Siegbahn PEM (1984) Chem Phys Lett 109:417
19. Olsen J, Roos BO, Jørgensen P, Jensen HJAa (1988) J Chem Phys 89:2185; Zarrabian S, Sarma CR, Paldus J (1989) Chem Phys Lett 155:183; Harrison RJ, Zarrabian S (1989) Chem Phys Lett 158:393